Spectral investigation of R, Ce:YAG (R: Pr^{3+}, Eu^{3+}, Gd^{3+}) single crystals and their applications in white LEDs

Du Yong(杜 勇)[a], Shao Chong-Yun(邵冲云)[a], Dong Yong-Jun(董永军)[b]†, Yang Qiu-Hong(杨秋红)[a], and Hua Wei(华 伟)[b]

[a] School of Materials Science and Engineering, Shanghai University, Shanghai 200072, China

[b] Key Laboratory of Materials for High Power Laser, Shanghai Institute of Optics and Fine Mechanics, Chinese Academy of Sciences, Shanghai 201800, China

(Received 22 April 2015; revised manuscript received 5 June 2015; published online 9 October 2015)

Eu^{3+}, Pr^{3+}, or Gd^{3+} codoped Ce:YAG single crystals were grown by using the Czochralski method. The photoluminescence (PL) emission and excitation spectra and transmittance were measured and investigated. The additional red-emitting bands were observed in the PL emission spectra of Eu,Ce:YAG and Pr,Ce:YAG single crystals and the formation of noticeable peaks was studied with reference to the schematic energy level diagrams. A red-shifted phenomenon was observed in the PL emission spectrum of Gd,Ce:YAG. With codoped Eu^{3+}, Pr^{3+}, or Gd^{3+} ions, warmer white light was achieved for the white light emitting diodes and the color rendering index became higher.

Keywords: photoluminescence, light-emitting device, electroluminescence

PACS: 78.55.–m, 85.60.Jb, 78.60.Fi **DOI:** 10.1088/1674-1056/24/11/117801

1. Introduction

With the continuous development of the light emitting diode (LED) manufacturing technology and growing demand in power LED applications, requirements of LED materials and devices with high luminous efficiency, low color temperature, and high color rendering index have been put forward. The method of yellow phosphor powders/blue chip to achieve white light has attracted much attention since Japan's Nichia first developed this technology. Owing to its simple makeup and easy packaging progress, this method has been adopted for the commercial application around the world and has been the focus of research.

However, the yellow silicone layer is observed with yellow phosphor and silicone glue long-time heating, leading to the shift of the color temperature.[1] Furthermore, the structure of the phosphor powders/blue chip is difficult to meet the requirement of low color temperature and high color rendering index for general lighting devices. In comparison, the Ce:YAG single crystal phosphor is a promising substitution for Ce:YAG powders, because of its optical transmittance, good photo-uniformity, and simple packaging progress. However, due to Ce:YAG phosphor emission peak centered at around 528 nm and short of red irradiation, high correlated color temperature (CCT) and low color rendering index (CRI) of Ce:YAG-based white LED are never meeting the requirement of light device applications. In order to solve the problem, some authors proposed adding a red-emitting phosphor layer to the surface of the yellow-green emitting phosphor layer.[2,3] For the Ce:YAG phosphors, it does not work because resin silicones must be used and thus it loses the original idea of resin-free package. The second approach is to codope using rare-earth ions that can enhance red emission, such as Cr^{3+}, Pr^{3+}, Eu^{3+}, Sm^{3+}, and Mn^{3+}.[4–7] Wang *et al.* reported the Cr enriched red emission and confirmed the nonradiative energy transfer from the Ce^{3+} level to the Cr^{3+} level in Ce,Cr:YAG.[8] Another paper showed the detailed white light optical indexes and made the color rendering index high to 80.1, but the intensity of their photoluminescence spetra was too low.[9] Though Cr^{3+} ions have a superior long red emission band ranging from 650 nm to 720 nm, the transmittance of the doped bulk crystal is always a big problem that impacts the optical properties. For Sm^{3+} ions, the optical properties of the related WLED cannot get obviously improved because the red emitting band is so weak at the blue light excitation. In this work, Eu^{3+}, Pr^{3+}, and Gd^{3+} ions were chosen as codoped ions in the Ce:YAG single crystal system. Detailed discussion was focused on the red-enhanced mechanism between Ce^{3+} and R^{3+} (Pr^{3+}, Eu^{3+}, Gd^{3+}) ions through the photoluminescence (PL) excitation and emission spectra. At the same time, the corresponding WLEDs were packaged and electroluminescent behaviors were investigated by comparison between R, Ce:YAG (R: Pr^{3+}, Eu^{3+}, Gd^{3+}) and Ce:YAG single crystal.

2. Experiment

2.1. Synthesis of R, Ce:YAG (R: Pr^{3+}, Eu^{3+}, Gd^{3+}) single crystal

The R, Ce:YAG (R: Pr^{3+}, Eu^{3+}, Gd^{3+}) single crystals were grown by the Czochralski method. The high-purity yttrium oxide powder (99.999%), aluminum oxide (99.999%), cerium oxide (99.99%) were uniformly mixed at the stoichio-

†Corresponding author. E-mail: dongyj@siom.ac.cn

© 2015 Chinese Physical Society and IOP Publishing Ltd

metric ratio and then pressed into blocks that placed in an iridium crucible. To grow the *R*, Ce:YAG (*R*: Pr^{3+}, Eu^{3+}, Gd^{3+}) single crystal, the oxide of *R* (praseodymium oxide, europium oxide, and gadolinium oxide) as a plus was added into the mixture. In our experiment, the concentrations of R^{3+} and Ce^{3+} were set as 0.8 mol% and 0.8 mol%, respectively. After molten at 1200 °C for 10 h in the Ar atmosphere to rule out the absorbent water and other impurities, the (111) oriented YAG single crystal used as a seed was gradually lifted up from the surface of the melting liquid. Through the periods of necking down, shoulder pulling, fixed-neck growing, and growing ending, a crystal was obtained. During fixed-neck growing, the lifting speed of the YAG single crystal seed was 1–2.5 mm/h with a spinning rate of 12 r/min.

2.2. Measurement

The crystalline phases of the samples were identified by x-ray diffraction (XRD) measurement (Bruker D8, Germany) using Cu K_α radiation. The absorption and transmittance spectra of all samples were tested with a spectrophotometer (Lambda950, Perkin Elmer). The emission and excitation spectra were recorded at the wavelength range of 200–750 nm, respectively, with a spectrophotometer equipped with a xenon lamp (JASCO FP6500, Japan).

The luminescent properties of all samples were tested by using a photo-electric testing system (PMS-80V1, EVERFINE). PMS-80V1 is an optical measurement system which contains an integrated sphere and a spectrometer, and controlled by a PC program. The LED chip was placed at the center of a reflector cup. The integrated sphere equipped with an optical fiber and a CCD detector was used to measure the optical spectrum of the WLED. When testing, the Ce:YAG single crystal plates were covered on the LED chip at the center of the integrated sphere. The scanning range was from 380 nm to 800 nm with the scanning interval of 5 nm and the input voltage of 3 V. The electroluminescence (EL) spectra, color coordinates, color rendering indexes, color temperatures, and luminous efficiencies of the specimens were tested.

3. Results and discussion

3.1. XRD analysis and optical transmittance of *R*, Ce:YAG (*R*: Pr^{3+}, Eu^{3+}, Gd^{3+}) single crystal

The XRD patterns of the Ce:YAG and *R*, Ce:YAG (*R*: Pr^{3+}, Eu^{3+}, Gd^{3+}) single crystals are shown in Fig. 1. The YAG single phase is identified, and weak peaks are observed which do not belong to the YAG phase, it is speculated that they are induced by crystal field splitting after the R^{3+} ions are codoped. The XRD pattern of the Ce:YAG single crystal is consistent with JCPDS card (No. 33-0040), indicating that the Ce^{3+} dopants are incorporated into the YAG host lattice without altering the original structure of YAG. Though the codoped ions induce weak peaks, they do not change the whole crystal structure and impact the following optical properties.

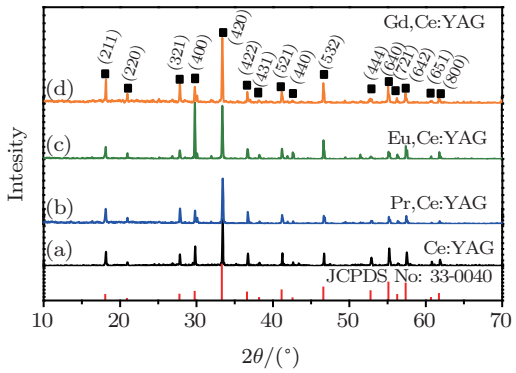


Fig. 1. (color online) XRD patterns of *R*, Ce:YAG (*R*: Pr^{3+}, Eu^{3+}, Gd^{3+}) single crystals.

The optical transmittances of the *R*, Ce:YAG (*R*: Pr, Eu, Gd) single crystals are shown in Fig. 2. The transmittance of the Eu,Ce:YAG single crystal sample is 79.66%, and those of the Gd,Ce:YAG and the Pr,Ce:YAG single crystal samples are 74.22% and 60.67% at 800 nm, respectively. The transmittance of the *R*, Ce:YAG (*R*: Gd^{3+}, Eu^{3+}) single crystal is obviously larger than that of the Pr,Ce:YAG single crystal. The absorptions at nearly 340 nm and 460 nm of all samples are generated by the absorption due to the corresponding Ce^{3+} transitions of $2F_{5/2} \rightarrow 5d$ and $2F_{7/2} \rightarrow 5d$, and those at 288 nm and 236 nm originate from the Pr^{3+} transitions of $4f^2 \rightarrow 4f5d$. The peak at 224 nm is attributed to the charge transfer band and the absorption at 275 nm corresponds to $^8S_{7/2} \rightarrow {}^6I_J$ of Gd^{3+}.

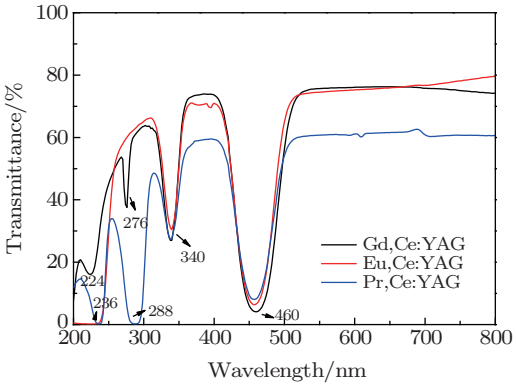


Fig. 2. (color online) Optical transmittances of *R*, Ce:YAG (*R*: Pr^{3+}, Eu^{3+}, Gd^{3+}) single crystals.

3.2. PL property of Eu,Ce:YAG single crystal

Eu^{3+} and Ce^{3+} simultaneously exist in the YAG crystal structure and the new ions system must be considered and discussed because of the interaction between the two ions. On one hand, the Ce^{3+} ion ($[Xe]^4f_1$) is likely to form the stable Xe electron configuration after losing one electron. On the other hand, the half-filled-shell effect will occur in the Eu^{3+} ion ($[Xe]^4f_6$) if an electron is obtained, which is the relatively stable electron configuration. Therefore, the chemical reaction

Eu^{3+} + Ce^{3+} →Eu^{2+} + Ce^{4+} is possible and there is doubt whether the Eu^{2+} ions are dominant in the YAG crystal structure. Fadlalla *et al*. studied the crystalline YAG:Eu^{2+} phosphors and the samples exhibited blue emission spectra within the range of 447–503 nm with the main broad-band emission peak at 480 nm, belonging to the characteristic emission of the $^4f_6^5d_1 \rightarrow {}^4f_7$ transition of Eu^{2+} ions in YAG.[10] However, it is not observed in the PL emission spectra of the Eu,Ce:YAG single crystal. So the effect of Eu^{2+}could be ignored. The PL emission spectra of the Eu,Ce:YAG single crystal under the excitation of 400 nm and 460 nm are shown in Fig. 3. Like the Ce:YAG single crystal, strong emission is observed around 527 nm, characteristic of the 5d→4f transition of the Ce^{3+} ion. With the detected wavelength of 530 nm, broad excited peaks at 466 nm and 341 nm are also shown along with the sharp excited peak at 263 nm in Fig. 4. The broad peaks centered at 466 nm and 341 nm are originating for the Ce^{3+} transitions of $2F_{5/2} \rightarrow$5d and $2F_{7/2} \rightarrow$5d. However, the strong-intensity light of wavelength 263 nm cannot directly excite the Ce^{3+} ions and we speculate that it belongs to the Eu^{3+} excitation from $^7F_0$ to upper F levels. Hence it is inferred that the energy transfer of $Eu^{3+} \rightarrow Ce^{3+}$ may take place in the Eu,Ce:YAG single crystal system. Enhancing the 528 nm emission band may be realized in two ways. In one way, the emission peak around 528 nm related to the Eu^{3+} transition from the $^5D_{1.2}$ level to the $^7F_{0.1.2}$ level directly appears after the Eu^{3+} non-radiative energy transition from the upper F levels to the $^5D_{1.2}$ level. In the other way, under the excitation of wavelength 263 nm, the Eu^{3+} ion is excited to the upper F level by optical excitation, then all of the energy is transferred to the 5d level of Ce^{3+}. The $^2D_{5/2} \rightarrow {}^2F_{5/2.7/2}$ transitions occur after the Ce^{3+} non-radiative transition 5d→$^2D_{5/2}$.

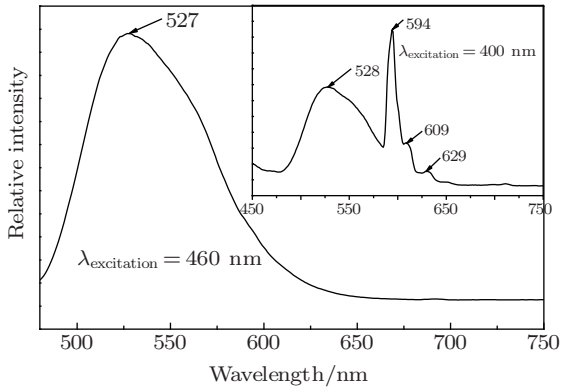


Fig. 3. PL emission spectrum of Eu,Ce:YAG single crystal after 460 nm excitation. The inset shows the PL emission spectrum corresponding to 400 nm excitation.

With codoped Eu^{3+} ions, we expect to see the Eu^{3+} contribution to enhance the red light wave band. Though the broad peak around 528 nm is obtained at the excitation of 460 nm, but this is the expected result. Therefore 400 nm is used as the excited wavelength, and the appearance of peaks at 528 nm, 594 nm, 609 nm, and 629 nm is depicted in the inset spectrum of Fig. 3. The intense emission peak at 594 nm, characteristic of Eu^{3+} magnetic dipole transition $^5D_0 \rightarrow {}^7F_1$, is found along with two relatively weak emissions around 609 nm and 629 nm, which are originating from Eu^{3+} electric dipole transitions of $^5D_0 \rightarrow {}^7F_2$ and $^5D^0 \rightarrow {}^7F_3$, respectively. The excitation spectrum corresponding to 590 nm emission is shown in Fig. 4. Except for the Ce^{3+} characteristic peaks, a tense peak centered at 294 nm can be clearly observed from the PL excitation spectrum. At the same time, the wavelengths around 341 nm and 460 nm cannot directly excite the Eu^{3+} ions but several red emission peaks are observed. The above various factors are taken into consideration, the energy transfer of $Ce^{3+} \rightarrow Eu^{3+}$ may happen in the the Eu,Ce:YAG single crystal system. That is to say, the excitation of Eu^{3+} occurs via the Ce^{3+} absorption, which means that the Ce^{3+} ion acts as a sensitizer for the Eu^{3+} luminescence. The energy transfer route of $Ce^{3+} \rightarrow Eu^{3+}$ can be deduced from the energy level diagrams for Ce^{3+} and R^{3+} ions (Fig. 7). The Ce^{3+} ion is excited to the $^2D_0$ (5d) state by optical excitation, then all of the energy is transferred to the $^5D_1$ level of Eu^{3+}. The $^5D_0 \rightarrow {}^7F_{1.2.3}$ transitions occur after the non-radiative transition $^5D_1 \rightarrow {}^5D_0$.

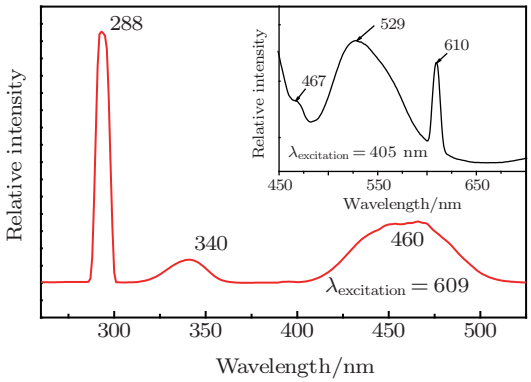


Fig. 4. (color online) PL excitation spectrum of Eu,Ce:YAG single crystal (detected wavelength of 590 nm). The inset shows PL excitation spectrum corresponding to detected wavelength of 530 nm.

3.3. PL property of Pr,Ce:YAG single crystal

Due to the Pr^{3+} abundant wave band for absorption and emission, it is believed that the Pr^{3+} ions are appropriate to be added to the Ce:YAG single crystal as a co-doping element for approving the emission light. Heesun Yang *et al.* reported the PL emission spectra of Pr-codoped YAG:Ce nanocrystalline samples with excitation wavelengths of 287 nm and 440 nm and the energy transfer between Pr^{3+} and Ce^{3+} was described.[6,7] Kim *et al.* introduced the single phase full-color-emitting phosphor for near-UV pumped white LED, but few studies on the codoped Ce:YAG single crystal using rare-earth ions have been reported.[11] The theoretical investigations on the codoped YAG:Ce nanocrystalline is almost based

on the crystal structure; to some degree, those theories can be applied to the codoped YAG:Ce single crystal.

Since excitation wavelengths of 287 nm and 440 nm have been studied, those of 385 nm, 405 nm, and 460 nm are chosen for the broad absorption in the Pr,CeYAG single crystal system in this paper. In order to investigate the formation of the emission peaks, wavelengths of 560 nm, 609 nm, and 696 nm are detected (520 nm and 608 nm corresponding excitation spectra in Ref. [6]). With the excitation of 385 nm, the Pr,CeYAG single crystal sample shows a sharp emission peak at 579 nm, which is related to the relaxation of $^3P_0 \rightarrow {}^3H_5$ of the Pr^{3+} ions. A broad emission peak at 529 nm and a sharp emission peak at 609 nm are observed under the excitation of 405 nm and 460 nm, but stronger in the former and weaker in the latter in comparison to the results under 440 nm in Ref. [6]. The appearance of the emission peaks at 529 nm and 609 nm is closely related to the $Ce^{3+} \rightarrow Pr^{3+}$ energy transfer. The $Ce^{3+} \rightarrow Pr^{3+}$ energy transfer can be depicted by a non-radiative relaxation and the radiative relaxation of the excited 5d electrons of the Ce^{3+} ion. After the electrons of the Ce^{3+} ion are excited from the 4f state to the 5d level, most of them return to the ground state of the Ce^{3+} ion, a small amount of them can transfer energy in the form of radiative relaxation from the 5d level to $^1D_2$ level of the Pr^{3+} ions. Another small amount of electrons can transfer nonradiative energy to the $^3P_0$ energy level of the Pr^{3+} ions. Consequently, 608 nm emission appears due to the radiative energy transition from the $^1D_2$ energy level to the $^3H_4$ energy level of the Pr^{3+} ions. The nonradiative way strengthens the emission in the range of 525–600 nm. Because 288 nm excitation cannot directly excite the Ce^{3+} ion existing in the Pr,Ce:YAG single crystal sample, the $4f_2 \rightarrow 4f5d$ transition is generated in the Pr^{3+} ions. Then the $Pr^{3+} \rightarrow Ce^{3+}$ energy transfer is realized in a nonradiative way which is the relaxation from the $^3P_0$ energy level of the Pr^{3+} ions to the 5d state of the Ce^{3+} ions, followed by the relaxation of the excited 5d electrons of the Ce^{3+} ions.

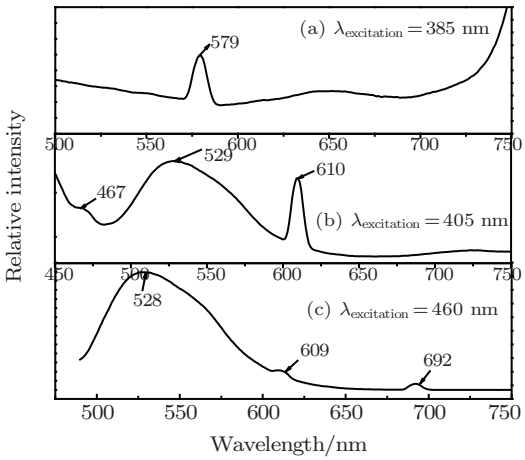


Fig. 5. PL emission spectra of Pr,Ce:YAG single crystal under excitation of various wavelengths: (a) 385 nm, (b) 405 nm, (c) 460 nm.

In addition, the small emission peak at 467 nm under the excitation of 405 nm and 692 nm are showed in Figs. 5(b) and 5(c). the former is originated from the transition of $^3P_0 \rightarrow {}^3H_5$ of the Pr^{3+} ions and the latter is corresponding to the radiative energy transition of $Ce^{3+} \rightarrow Pr^{3+}$, followed by the $^1D_2$ level to ^2F level of the Pr^{3+} ions. Figure 6(c) shows the PL excitation with detected wavelength of 695 nm, and only an excited peak at 460 nm is observed. As the Pr^{3+} ions cannot be directly excited by the excitation of wavelength 460 nm, the result reflects the $Ce^{3+} \rightarrow Pr^{3+}$ energy transfer.

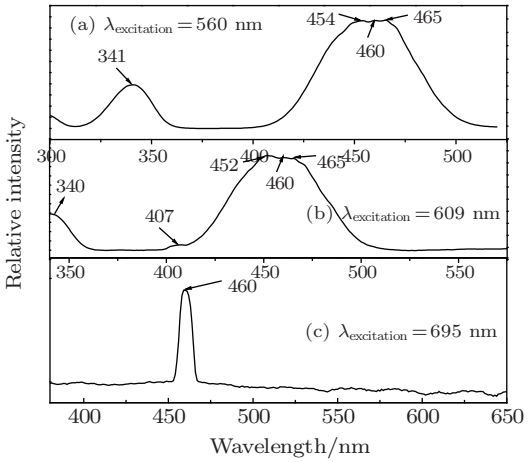


Fig. 6. PL excitation spectra of Pr,Ce:YAG single crystal with various detected wavelengths: (a) 560 nm, (b) 609 nm, (c) 695 nm.

3.4. PL property of Gd,Ce:YAG single crystal

As can be seen in the schematic energy level diagrams of Ce^{3+} and Gd^{3+} ions (Fig. 7), the 6P level of the Gd^{3+} ion is partly overlapped with the 5d level of the Ce^{3+} ion. The energy transfer is able to occur between Gd^{3+} and Ce^{3+} ions in theory. However, most researchers did not pay attention to the energy level transition, because the Gd^{3+} ion did not induce other longer emission wave bands. In recent years, the Gd^{3+}-substituted Ce:YAG phosphors have been intensively studied due to its special spectral variation. Yang *et al.* reported that the Ce^{3+} emission was red-shifted by Gd^{3+} substitution due to a modified crystal field splitting in the Gd,Ce:YAG nanocrystalline system.[7] Nishiura *et al.* studied the high power application in white LEDs using transparent Gd,Ce:YAG ceramics.[12] While for the single crystal, only Latynina *et al.* reported the properties of Czochralski grown Ce,Gd:$Y_3Al_5O_{12}$ single crystal for white light-emitting diode and the corresponding wafers showed better values and improved stability under high temperatures in comparison to the commercial phosphor powders.[13] In this paper, compared with those of Ce:YAG, Eu,Ce:YAG, and Pr,Ce:YAG single crystals, the PL emission of Gd,Ce:YAG under the excitation of 340 nm and 460 nm is depicted in Figs. 8 and 9. The emission spectra of Ce:YAG, Eu,Ce:YAG, and Pr,Ce:YAG single crystals at 528 nm are almost overlapped in Fig. 8, and with

the codoped Gd^{3+} ion, the related emission spectra are red-shifted 13 nm to the emission peak at 541 nm. In Fig. 9, for the PL emission of the Pr^{3+} and Eu^{3+} codoped Ce:YAG single crystal, the red-shift spectral peak changes from 528 nm to 531 nm and it is not obvious. However, the width of the emission band is enlarged and it is beneficial to improve the luminescent behaviors of the corresponding devices. For the PL emission of the Gd,Ce:YAG single crystal, the broad band emission is red-shifted from 528 nm to 540 nm. It coincides with Nishiura *et al.*'s report. According to Ref. [14], the 5d state of the Ce^{3+} ion can be adjusted by partially substituting Y^{3+} or Al^{3+} site with different types of cations. Because the ionic radius of Gd^{3+} (1.05 Å) is larger than that of Y^{3+} (1.02 Å) occupying a dodecahedral site in the host lattice of the YAG single crystal, the substitution of the Gd^{3+} ion causes the Ce–O distance to be shortened, leading to an increased crystal field splitting. It is noted that the crystal field splitting (D_q) is proportional to $\sim 1/r^5$, where r is the bond length of the activator cation–ligand anion. This larger crystal field splitting further lowers the lowest energy level of the Ce 5d state band and consequently induces a red-shift of the Ce emission. The electroluminescent behaviors are investigated in the following.

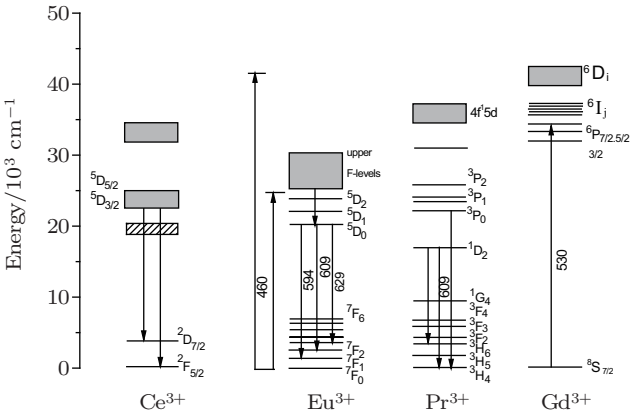


Fig. 7. Schematic energy level diagrams of Ce^{3+}, Eu^{3+}, Pr^{3+}, and Gd^{3+} ions.

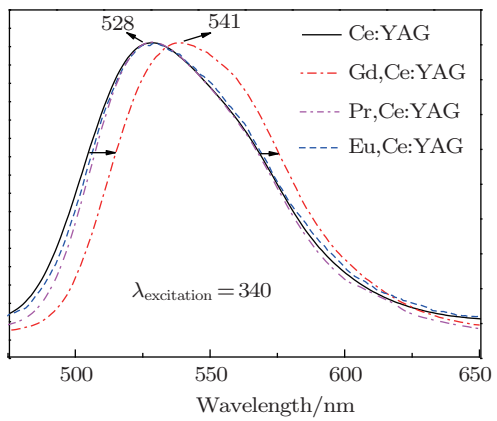


Fig. 8. (color online) The PL emission spectra of *R*, Ce:YAG (*R*: Pr^{3+}, Eu^{3+}, Gd^{3+}) single crystals under 340 nm excitation.

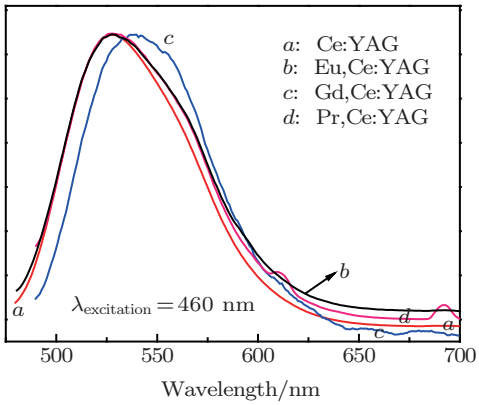


Fig. 9. (color online) The PL emission spectra of *R*, Ce:YAG (*R*: Pr^{3+}, Eu^{3+}, Gd^{3+}) single crystals under 460 nm excitation.

3.5. Properties of blue-InGaN-chip-based WLEDs utilizing *R*, Ce:YAG (*R*: Pr^{3+}, Eu^{3+}, Gd^{3+}) single crystal

The excitation band covering from 400 nm to 500 nm is most intense and provides a background for the application of these phosphors in blue InGaN chips. The broad band located from 500 nm to 600 nm provides an ideal yellow light complementary to the blue light emitted by InGaN LED chips to produce white light. Here we choose the 460 nm-LED chips as a basis to improve the electroluminescent properties of WLEDs utilizing *R*, Ce:YAG (*R*: Pr^{3+}, Eu^{3+}, Gd^{3+}) in comparison to the Ce:YAG-based WLED.

When the thickness of the sample is 1 mm, the Ce:YAG-single-crystal-based WLED shows a high luminous efficiency (42.45l m/W) and a color rendering index of 62.8 (Table 1). And it produces a natural white light (5030 K). The Eu,Ce:YAG-single-crystal-based WLED displays a relatively lower luminous efficiency (22.11l m/W) and a color rendering index of 72.9, which gives a cold white light (6777 K). At the same time, the Pr,Ce:YAG-single-crystal-based WLED gives a higher luminous efficiency of 45.86 lm/W, which is almost 2.5 times of that in Ref. [7], and shows a warm white light (4420 K). With the Gd^{3+} codoped Ce:YAG single crystal, the corresponding WLED shows a luminous efficiency of 41.29l m/W and produces the warmest white light (3663 K). These statistics indicates that via codoping R^{3+} (Eu^{3+}, Pr^{3+}, Gd^{3+}) ions in the Ce:YAG single crystal system, the electroluminescent properties of the related WLEDs can be improved with higher color rendering index and warmer white light.

Table 1. Optical properties of white LEDs using 1.0-mm-thickness *R*, Ce:YAG (*R*: Pr^{3+}, Eu^{3+}, Gd^{3+}) single crystals at the current of 250 mA.

Sample	CRI	LE/lm·W^{-1}	CCT	CIE(x, y)
Ce:YAG	62.8	42.45	5030	(0.3525, 0.4483)
Eu,Ce:YAG	72.9	22.11	6777	(0.3039, 0.3511)
Pr,Ce:YAG	62.6	45.86	4420	(0.3875, 0.4900)
Ce,Gd:YAG	60.5	41.29	3663	(0.4252, 0.4707)

The same result can be concluded from Fig. 10. Figure 10 exhibits the thickness-dependent CIE color coordinates of all

as-prepared samples. With the thickness increasing, the CIE x and y values increase and the corresponding points move greatly from the blue region to the yellow-greenish region. For certain kinds of materials (such as Ce:YAG single crystal), the corresponding points are approximately linearly distributed. So we use lines *a*–*d* respectively to represent the CIE color coordinates related to all thicknesses of *R*, Ce:YAG (*R*: 0, Eu^{3+}, Pr^{3+}, Gd^{3+}). The lines *b*–*d* shift to the more deeper yellow region than that of the Ce:YAG single crystal, which is caused by the strengthened red component light with the codoping ions. In particular, the point of the Gd^{3+} codoped Ce:YAG single crystal moves the deepest in the yellow region and causes a higher color temperature (warmer white light). This result is attributed to the red-shift phenomenon, the emission peak shifts to the longer wavelength with the codoping Gd^{3+} ions. The enhanced performance of Eu,Ce:YAG and Pr,Ce:YAG single crystals is due to the broadened emission peak at 528 nm and the additional red wave band.

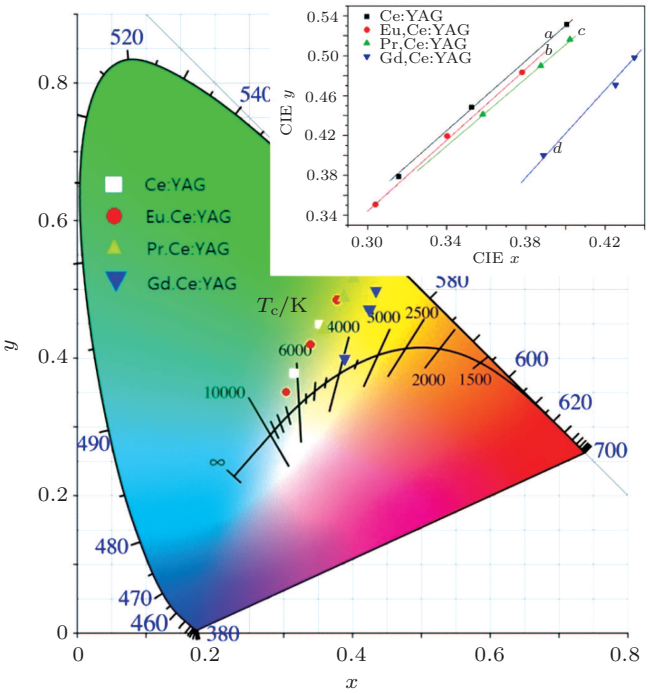


Fig. 10. (color online) The CIE color coordinates of WLEDs using *R*, Ce:YAG (*R*: Pr^{3+}, Eu^{3+}, Gd^{3+}) single crystals of different thicknesses (0.5 mm, 1.0 mm, 2 mm).

4. Conclusion

The spectral properties of yellow-emitting Ce:YAG single crystal phosphors were varied via codoping Eu^{3+}, Pr^{3+}, and Gd^{3+} ions. The characteristic peaks of Eu^{3+} at 528 nm, 594 nm, 609 nm, and 629 nm were observed under the excitation of 400 nm. The Ce^{3+} ion acts a sensitizer for the Eu^{3+} luminescence. The Ce^{3+} ion is excited to the $^2D_0$ (5d) state by optical excitation, then all of the energy is transferred to the $^5D_1$ level of Eu^{3+}. The $^5D_0 \rightarrow {}^7F_{1,2,3}$ transitions occur after the non-radiative transition $^5D_1 \rightarrow {}^5D_0$. The emission peaks at 528 nm and 609 nm were detected due to the $Ce^{3+} \rightarrow Pr^{3+}$ transition, in which the Ce^{3+} ion is used as a sensitizer, too. Red-emitting bands are abundant in the PL emission spectra of the Pr^{3+} codoped Ce:YAG single crystal system. A red-shifted phenomenon was observed in the PL emission spectrum of Gd,Ce:YAG due to the larger crystal field splitting. In comparison to the Ce:YAG single crystal, WLEDs utilizing Eu,Ce:YAG and Pr,Ce:YAG obtained relatively higher CRI of 72.9 and warmer white light (4420 K). The Eu,Ce:YAG-based WLED gave the warmest white light (3663 K) without losing luminous efficiency (41.29l m/W).

References

[1] Li B Q, Liu Y H and Feng Y C 2008 *Acta Phys. Sin.* **57** 477 (in Chinese)
[2] Jang H S, Won Y H and Jeon D Y 2009 *Appl. Phys. B* **95** 715
[3] Aboulaich A, Michalska M, Schneider R, Potdevin A, Deschamps J, Deloncle R, Chadeyron G and Mahious R 2014 *ACS Appl. Mater.* **6** 252
[4] Zorenko Y, Voznyak T, Vistovsky V, Zorenko T, Nedilko S, Batentschuk M, Osvet A, Winnacker A, Zimmerer G, Kolobanav V and Spassky D 2007 *Radiat. Meas.* **42** 648
[5] Wang L, Zhang X, Hao Z, Luo Y S, Wang X J and Zhang J H 2010 *Opt. Express* **28** 25177
[6] Yang H and Kim Y S 2008 *J. Lumin.* **128** 1570
[7] Yang H, Lee D K and Kim Y S 2009 *Mater. Chem. Phys.* **114** 665
[8] Wang W D, Tang J K, Hsub S T, Wang J and Sullivan B P 2008 *Chem. Phys. Lett.* **457** 103
[9] Wang X, Zhao G J and Chen J Y 2011 *Chin. J. Lasers* **48** 101601
[10] Fadlalla H M H, Tang C C, Elssfah E M and Shi F 2008 *Mater. Chem. Phys.* **109** 436
[11] Kim J S, Jeon P E, Choi J C, Park H L, Mho S I and Kim G C 2004 *Appl. Phys. Lett.* **84** 2931
[12] Nishiura S, Tanabe S, Fujioka K, Fujimoto Y and Nakatsuka M 2011 *IOP Conference Series: Materials Science and Engineering* **18** 102005
[13] Latynina A, Watanabe M, Inomata D, Aoki K, Sugahara Y, Villora E G and Shimamura K 2013 *J. Alloys Compd.* **553** 89
[14] Jang H S, Im W B, Lee D C, Jeon D Y and Kim S S 2007 *J. Lumin.* **126** 371